A Letters Journal Exploring the Frontiers of Physics

January 2009

EPL, **85** (2009) 27004
doi: 10.1209/0295-5075/85/27004

www.epljournal.org

Observation of surface superconductivity and direct vortex imaging of a Pb thin island with a scanning tunneling microscope

Y. X. Ning[1], C. L. Song[1,2], Z. L. Guan[1], X. C. Ma[1(a)], Xi Chen[2], J. F. Jia[2] and Q. K. Xue[1,2(b)]

[1] *Institute of Physics, The Chinese Academy of Sciences - Beijing 100190, China*
[2] *Department of Physics, Tsinghua University - Beijing 100084, China*

received 7 November 2008; accepted in final form 17 December 2008
published online 30 January 2009

PACS 74.25.Op – Mixed states, critical fields, and surface sheaths
PACS 74.25.Qt – Vortex lattices, flux pinning, flux creep
PACS 68.37.Ef – Scanning tunneling microscopy (including chemistry induced with STM)

Abstract – We report on a scanning tunneling spectroscopy study on vortex imaging and surface superconductivity of a thin type-II superconducting Pb island, which is epitaxially grown on Si substrate and 12 atomic monolayers in thickness. The field dependence of vortex lattice evolution reveals the existence of the surface superconducting layer, which is parallel to the magnetic field in the periphery of the island and disappears above a critical field H_{c3} of 3077 G. The H_{c3}/H_{c2} ratio of 1.57 gives a further support for the surface superconductivity.

When a magnetic field H is applied to a type-II superconductor such as a Pb thin film, the vortices each carrying a single flux quantum $\Phi_0(2.07\times10^{-7}\,\mathrm{G\cdot cm^2})$ will appear in the form of a hexagonal lattice with a vortex spacing $d=(2\Phi_0/\sqrt{3}H)^{1/2}$ [1]. In the core of a vortex, superconductivity is suppressed within a radius of the same order of the coherence length ξ. At a magnetic field just above the upper critical field H_{c2}, the bulk of the superconductor goes to the normal state. However, the superconducting state can still exist in a thin layer at the edge of specimen even in much higher fields. The thickness of this surface superconducting layer is of the order of ξ and will be destroyed at the third critical field $H_{c3}(>H_{c2})$. From the linear Ginzburg-Landau (GL) equation for isotropic materials, a universal value 1.6946 for the ratio H_{c3}/H_{c2} can be obtained [2], which has stimulated extensive studies on the onset of superconductivity in higher fields in the past decades [3–7]. So far, the evidences of surface superconductivity had been shown only by transport measurements [3,4,7] and theoretical calculations [5,6]. Here, we report the real-space observation of the surface superconductivity by means of low-temperature high-magnetic-field scanning tunneling microscopy/spectroscopy (STM/STS).

STS is a powerful technique to detect the structure of individual vortex as well as the electronic states within the vortex cores. It has been employed to image vortex lattices of many compounds, such as $NbSe_2$, MgB_2, YBa_2CuO, $LuNi_2B_2C$ [8–13]. As for a type-II elementary superconductor [14–17], magnetic field dependence and spatial distribution of superconductivity in nanosized Pb islands (<75 nm in radius) were studied most recently, and vortex formation was observed in the Pb island with a minimum lateral size of 48 nm [18]. However, no STM/STS study on vortex lattice evolution has so far been performed on Pb. Note that bulk Pb is a type-I superconductor with a critical field (H_c at 0 K) of 800 G, a relatively high superconducting transition temperature (T_c) of 7.2 K and a BCS coherence length (ξ_0) of 83 nm.

In our study, crystalline Pb(111) islands with a large size of about 300 nm in radius were used as our samples. These islands have been well characterized in our previous study [19,20]. In this study, by using low-temperature STM/STS with high magnetic field, the formation of the vortex lattice and its evolution are investigated in detail. Moreover, zero-bias conductance (ZBC) maps under different magnetic fields reveal the existence of the surface superconducting layer on the island edge. To the best of our knowledge, this is the first real-space observation of surface superconductivity in a low-dimensional superconducting system.

(a) E-mail: xcma@aphy.iphy.ac.cn
(b) E-mail: qkxue@mail.tsinghua.edu.cn

Our experiments were performed in an ultrahigh vacuum (UHV) low-temperature STM system combined with a molecular-beam-epitaxy (MBE) chamber (Unisoku USM-1300 and RHK SPM 1000). This allows us to prepare and characterize samples under *in situ* UHV conditions. Pb(111) islands were grown by depositing high-purity (99.999%) Pb from a Knudsen cell onto the Si(111)-7×7 substrate (As-doped, $1-5\,\mathrm{m\Omega\cdot cm}$) while keeping the vacuum better than 2×10^{-10} torr [19,20]. In order to grow a uniform-height island, a step-bunched surface for the Si substrate was purposely prepared, on which large terraces of more than 300 nm wide were often observed [21]. After Pb growth, the sample was transferred in UHV into the STM stage for STM/STS measurements. During STM observation, the sample temperature was maintained at 4.32 K by liquid helium cooling. A magnetic field up to 7 tesla could be applied perpendicular to the sample surface if needed. The tunneling conductance spectra ($\mathrm{d}I/\mathrm{d}V$) were acquired using the standard lock-in technique with a small ac modulation of 0.2 mV, while the vortex images were obtained by taking STS mapping at different magnetic fields applied perpendicularly to the sample surface [8]. All measurements were carried out after zero-field cooling the sample to 4.32 K and using PtIr tips.

Figure 1(a) shows a typical STM image of a Pb island grown on the Si substrate. The island has an atomically flat (111) surface and a uniform thickness of 3.43 nm consisting of 12 atomic monolayers (MLs) above the Pb wetting layer. Note that an area of $350\,\mathrm{nm}\times350\,\mathrm{nm}$ is marked by a black square in fig. 1(a) for the following vortex imaging. Shown in fig. 1(b) is a typical $\mathrm{d}I/\mathrm{d}V$ *vs.* V tunneling spectrum without external field, which has been normalized by dividing every conductance data by that at high bias (green dotted curve). It displays a clear superconducting gap and can be reasonably fitted with the Dynes' expression including a broadening factor, which is due to the limited quasiparticle lifetime and the temperature effect (red curve) [16,22].

Vortex imaging is based on the difference in conductance curves inside and outside a vortex core when a magnetic field is applied. When the tip is positioned far away from the vortex core, the obtained spectrum is basically identical to that shown in fig. 1(b) with a clear superconducting gap at the Fermi energy ($V_{\mathrm{bias}}=0\,\mathrm{V}$). Inside a vortex core the superconductivity is suppressed, and therefore the tunneling conductance at zero bias exhibits an increase. To take an image of the vortex lattice in real space, we recorded the spatial variations of the zero-bias conductance at 64×64 points on the scanning region. As shown in fig. 2, a set of vortex images on the Pb island at different magnetic fields indicate the appearance of individual vortex and formation of vortex lattice. Note that, in the vortex images the superconducting regions of low conductance are marked with maroon color, while the gapless normal state regions inside the vortex core are yellow-colored. As the external magnetic field increases,

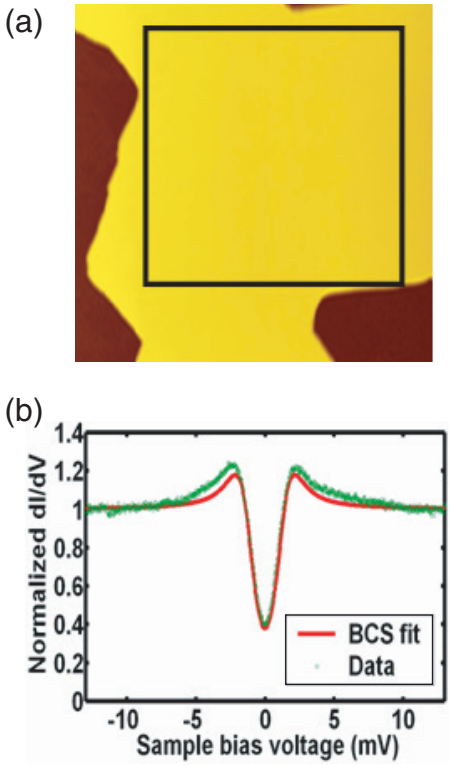

Fig. 1: (Color online) (a) STM image ($500\,\mathrm{nm}\times500\,\mathrm{nm}$) of a Pb thin island with a uniform height of 12 ML. The image was taken with a sample bias $V_{\mathrm{sample}}=3.0\,\mathrm{V}$ and a tunneling current $I_t=0.2\,\mathrm{nA}$. The region in the black square is $350\,\mathrm{nm}\times350\,\mathrm{nm}$, on which the vortex imaging was performed. (b) Zero-field tunneling conductance spectrum (the green curve) of the Pb island at 4.32 K. It is normalized to high bias conductance ($\pm12\,\mathrm{meV}$). The red curve is the fitting result by BCS theory, which yields a superconducting gap $\Delta=1.3\,\mathrm{meV}$ and the broading factor $\Gamma=0.4\,\mathrm{meV}$. The data was taken with a bias modulation $0.2\,\mathrm{mV_{rms}}$ at a frequency 2 kHz. The tunneling gap was set at $V_{\mathrm{sample}}=10\,\mathrm{mV}$ and $I_{\mathrm{t}}=0.2\,\mathrm{nA}$.

the distance between vortices decreases (see figs. 2(b) and (c)). At the second critical field, the cores merge together and most parts of the island go into the normal state (fig. 2(e)).

In the presence of a low magnetic field of 375 G (see fig. 2(a)), the intervortex distance $d=252\,\mathrm{nm}$ is three times larger than $\xi_0=83\,\mathrm{nm}$ of the bulk Pb. The vortices can therefore be considered as isolated from each other. Figure 3 shows a series of $\mathrm{d}I/\mathrm{d}V$spectra measured at the center of the isolated vortex, and 40 nm, 75 nm, 150 nm apart from the center, respectively. The spectrum taken at 150 nm from the core exhibits a clear superconducting gap, which is gradually suppressed when moving to the vortex center. At the core, the spectrum is flat without excess peak induced by the bound state of quasiparticles, contrary to the case of 2H-$NbSe_2$ [8]. The absence of ZBC peak at the vortex core indicates that the sample is in the dirty limit [23], which is due to the electronic mean free path (l) being smaller than the BCS coherence

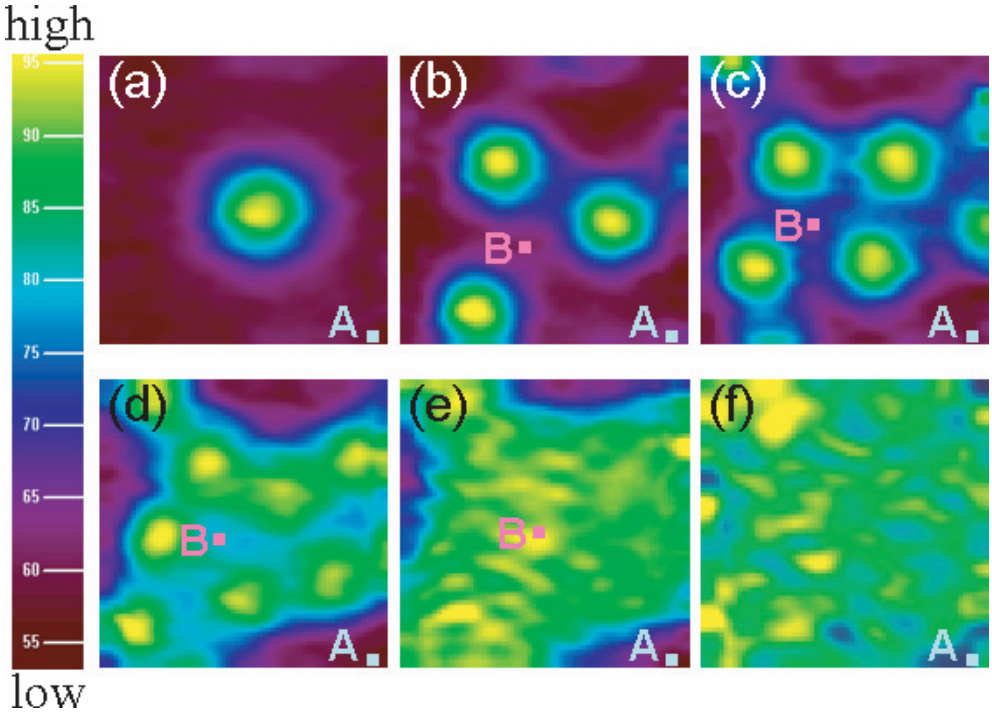

Fig. 2: (Color online) A series of vortex images on the Pb island at different magnetic fields of 375 G (a), 750 G (b), 1125 G (c), 1500 G (d), 2250 G (e), and 3000 G (f). They were taken from the same region (the square marked in fig. 1(a)). Markers A and B in the images are the measurement positions of the spectra shown in fig. 4.

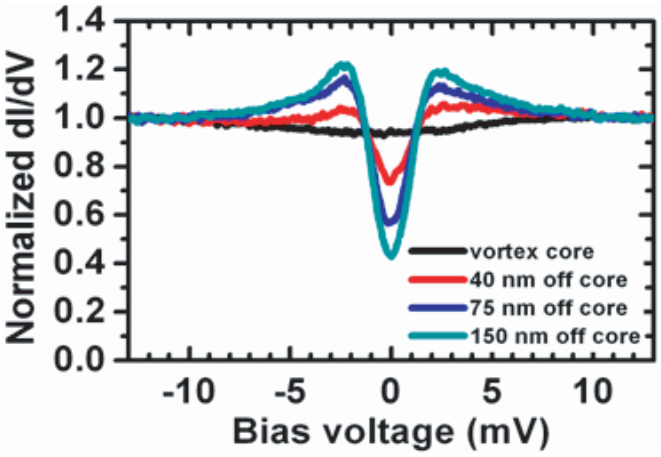

Fig. 3: (Color online) A series of $\mathrm{d}I/\mathrm{d}V$ spectra (normalized to high bias conductance (± 12 meV)) measured at the center of a vortex core, and 40 nm, 75 nm, 150 nm away from the center at 4.32 K and 375 G.

length. Reduction of the mean free path can be attributed to the strong scattering from the disorder of the wetting layer in thin films. This is consistent with other studies, where we have found that the sample becomes a clean superconductor when the film is thicker than 47 nm, resulting in a ZBC peak in the spectrum of vortex core. It is worth noticing that in our experiments, zero bias conductance measured at the normal state (the vortex core or high fields larger than H_{c3}) is slightly less than the high-bias conductance, as the black curve in fig. 3. This dip feature of the $\mathrm{d}I/\mathrm{d}V$ spectrum at normal state may be ascribed to the electron-phonon interaction in a thin film, in addition to the existence of the wetting layer under the Pb islands [18].

With increasing magnetic field, more vortices emerge, forming a quasi-hexagonal vortex lattice as shown in figs. 2(b) and (c) for $H = 750$ G and 1125 G, respectively. There is a clear overlapping of the vortex cores and a suppression of superconductivity in the regions between the vortices, which is confirmed by the ZBC increase as shown in fig. 4(b). It is well known that when a field H is applied to a type-II superconductor, the vortices are generally arranged in the form of a hexagonal lattice with a spacing $d = (2\Phi_0/\sqrt{3}H)^{1/2}$ and the area of a triangle formed by three nearest vortices is $A = \Phi_0/2H$. In the present case, the lattice is not well defined, which is probably due to the edge effect of the irregular-shaped Pb island. At 750 G, the area of the triangle formed by the three vortices (see fig. 2(b)) can be calculated as 12058 nm^2, which is smaller than the theoretical value of 13800 nm^2. Similar phenomenon is found in fig. 2(c) as well as all of other measurements. This suggests that the observed vortex density is denser than that predicted in theory, which will be addressed later.

Near the upper critical field, the distance between two neighboring vortices approaches to ξ_{GL}. In this case, the boundaries between vortices are nearly invisible at

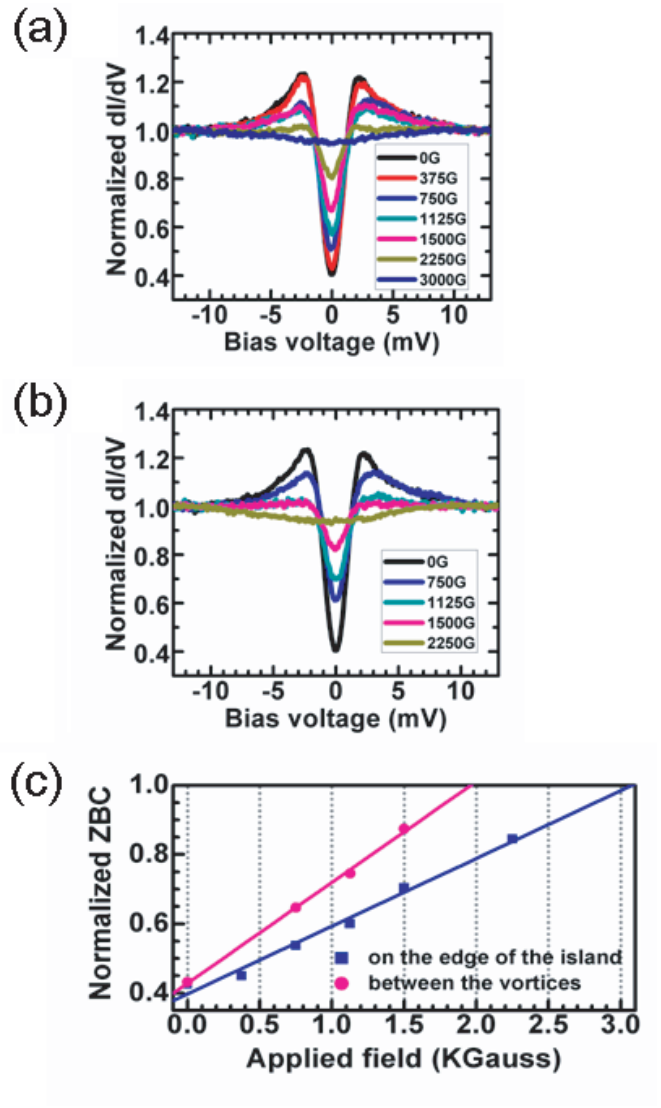

Fig. 4: (Color online) Magnetic-field dependence of normalized dI/dV spectra taken at the edge of the island (a) and between the vortices on the island (b). (c) Normalized ZBC measured at different fields (discrete symbols) and the corresponding linear fitting (lines).

1500 G (see fig. 2(d)). Interestingly, the periphery of the merged vortex region exhibits very similar shape as that of the island. When a field of 2250 G ($> H_{c2}$) is applied, except for each edge of the island (see fig. 2(e)), the rest of the island goes into the normal state, suggesting that there exists a surface superconducting layer close to the edge with a higher critical field. Above this field, even the surface superconductivity is destroyed, as seen in fig. 2(f). The field for breakdown of the surface superconductivity can be defined as H_{c3} accordingly. By comparing the vortex images in figs. 2(d), (e) and (f), a relationship of $1500\,\mathrm{G} < H_{c2} < 2250\,\mathrm{G} < H_{c3} < 3000\,\mathrm{G}$ could be obtained in such a island. Further analyzing the images (see figs. 2(e) and 1(a)), one can estimate the thickness of this surface superconducting layer. By repeatedly measuring the distance of blue region to the island edge at different locations, the average thickness of the superconducting layer is found to be 51.9 ± 6.1 nm. All these experiments substantially support the existence of a surface superconducting layer parallel to the field in the periphery of the island.

To accurately determine the critical field H_{c3} for surface superconductivity breaking, magnetic-field–dependent tunneling conductance measurements both on the edge of the island and between the vortices were carried out. Figures 4(a) and (b) show the spectra under magnetic fields ranging from 0 to 3000 G, which were taken at two positions (A and B) on the island surface, as marked in fig. 2, respectively. One can clearly see that the spectra taken on the island edge always exhibit a lower ZBC (deeper gap, site A) than those on the terrace (site B), in agreement with previous studies [1,2]. At 2250 G, the center of the island becomes the normal state, while the periphery of the island is still superconducting. At 3000 G, all the surface of the island becomes a normal metal. Similar with the black curve in fig. 3, the ZBC values at the normal state (at 3000 G and 2250 G in figs. 4(a) and (b), respectively) are 0.93 and 0.95, respectively, instead of 1, even though the applied field is already above H_{c3}. Fitting the data in figs. 4(a) and (b), a linear dependence of ZBC on the magnetic field is evidenced (see fig. 4(c)). Here, ZBCs on the edge of the island and between the vortices are all divided by the high field value, namely, 3000 G and 2250 G, respectively. There is no effect on the fitting result. The linear dependence of ZBC with the external field is predicted for superconducting spherical particles with smaller sizes than the coherence length ξ_0, according to a calculation using the Gor'kov equation [24]. In our study, the ZBCs at the peripheral site of Pb island (~ 300 nm in radius) and the center of vortices also increase monotonically with the field until saturation, similar to the study in ref. [18].

By extrapolating to the point where ZBC $= 1$ (*i.e.*, normal state), one can obtain the upper critical field of the interior H_{c2} and the island edge H_{c3}, which is 1960 G and 3077 G, respectively. Our fitted H_{c2} (1960 G) for 12 ML Pb island is quite reasonable, as compared to the result ($H_{c2} = 2100$ G for a 13 ML Pb thin film at 4.3 K) by using a superconducting quantum interference device magnetometer [25]. For H_{c3}, there is a slight difference between the fitted value (3077 G) and the field (3000 G) based on vortex observation (see fig. 2(f)), probably due to the superconductivity fluctuation near the critical field [1]. The ratio (H_{c3} to H_{c2}) is equal to 1.57 and very close to the theoretical value of 1.69, suggesting that a surface superconducting layer parallel to the field does exist at the edge of the Pb island. The reduced value by 7% can be attributed to the finite-temperature effect at 4.32 K [5].

In a dirty superconductor, the characteristic scale of inhomogeneity is the electronic mean free path and the GL theory applies if $\xi_{GL}(T), \lambda(T) \gg l$ [26]. The validity of the 3D GL analysis for this extreme 2D geometry was

demonstrated on 5–18 ML Pb thin films by Özer *et al.* [25,27]. Via the relation $H_{c2}(T) = \Phi_0/2\pi\xi^2_{\rm GL}(T)$ [1], the GL coherence length of $\xi_{\rm GL}(4.32\,{\rm K}) = 41\,{\rm nm}$ can be obtained in our experiment. Furthermore, the coherence length $\xi_{\rm GL}(0) \approx 21.7\,{\rm nm}$ at zero temperature for a 12 ML Pb film can be deduced by using the GL expression $\xi_{\rm GL}(T) = \xi_{\rm GL}(0)(1 - T/T_c)^{-1/2}$ [1], where $T_{\rm c}(12\,{\rm ML}) \approx 6.0\,{\rm K}$ (inferred from ref. [17]). This value is very comparable with the result for a 9 ML Pb film ($\xi_{\rm GL}(0) \approx 23\,{\rm nm}$) [27]. In addition, it is significantly smaller than BCS value of bulk Pb (83 nm), primarily due to the reduced mean free length in this two-dimensional system. Having deduced the coherence length, we can now estimate the scattering-increased penetration depth $\lambda_{\rm eff}$. According to the Anderson theorem [27,28], the product $(\lambda_{\rm L}\xi_0^{'})_{\rm bulk} \approx (\lambda_{\rm eff}\xi_{\rm GL})_{\rm film}$ is independent of scattering and thus film thickness, where $\lambda_{\rm L}$ is the London penetration depth of bulk Pb ($\sim 37\,{\rm nm}$) and $\xi_0^{'}$ is the BCS coherence length using $\xi_0^{'}T_{\rm c}^{\rm film} = \xi_0^{\rm bulk}T_{\rm c}^{\rm bulk}$. These formulae give $\lambda_{\rm eff} \approx 169.8\,{\rm nm}$ and $\kappa = \lambda_{\rm eff}/\xi_{\rm GL} \approx 7.8$, consistent with the behavior of a type-II superconductor.

Finally, we discuss the influence of the surface superconductivity on distribution of the vortex lattices in Pb islands. In general, the vortices on the island will repel each other. At the same time, the surface superconducting layer produces a repulsive force which pushes the vortex away from the island edge [26], resulting in a more dense distribution of vortices on the island, which was indeed observed in our experiment, as mentioned above. The balance of the two opposite interactions determines the spatial distribution of the vortices island-shaped, as observed in figs. 2(d) and (e). To verify this edge effect, we also performed vortex imaging on a uniform thin Pb film of much larger size. In this case, the measured vortex lattice fits the theoretical value well.

In summary, the vortex imaging of an elementary type-II superconductor under various magnetic fields was investigated by using low temperature STM/STS technique. The upper critical field $H_{\rm c2}$ and the GL coherence length in a 12 ML Pb island are determined as 1960 G and 41 nm, respectively. A surface superconducting layer is successfully observed in real space, which is parallel to the field in the periphery of the island and disappears above a critical field $H_{\rm c3}$ of 3077 G at 4.32 K. Those data will be valuable to the characterization of a low-dimensional superconducting system of the superconductivity community.

* * *

This work is financially supported by the National Natural Science Foundation and the Ministry of Science and Technology of China.

REFERENCES

[1] Tinkham M., *Introduction to Superconductivity*, 2nd edition (New York, McGraw-Hill) 1996.
[2] Saint-James D. *et al.*, *Phys. Lett.*, **7** (1963) 306.
[3] Strongin M. *et al.*, *Phys. Rev. Lett.*, **16** (1964) 442.
[4] Moshchalkov V. V. *et al.*, *Nature*, **373** (1995) 319.
[5] Agterberg D. F. *et al.*, *Phys. Rev. B*, **53** (1996) 15201.
[6] Kogan V. G. *et al.*, *Phys. Rev. B*, **65** (2002) 094514.
[7] Gorokhov D. A. *et al.*, *Phys. Rev. Lett.*, **94** (2005) 077004.
[8] Hess H. F. *et al.*, *Phys. Rev. Lett.*, **62** (1989) 214.
[9] Maggio-Aprile I. *et al.*, *Phys. Rev. Lett.*, **75** (1995) 2754.
[10] De Wilde Y. *et al.*, *Phys. Rev. Lett.*, **78** (1997) 4273.
[11] Eskildsen M. R. *et al.*, *Phys. Rev. Lett.*, **89** (2002) 187003.
[12] Sosolik C. E. *et al.*, *Phys. Rev. B*, **68** (2003) 140503(R).
[13] Bergeal N. *et al.*, *Phys. Rev. Lett.*, **97** (2006) 077003.
[14] Guo Y. *et al.*, *Science*, **306** (2004) 1915.
[15] Bao X. Y. *et al.*, *Phys. Rev. Lett.*, **95** (2005) 247005.
[16] Nishio T. *et al.*, *Appl. Phys. Lett.*, **88** (2006) 113115.
[17] Eom D. *et al.*, *Phys. Rev. Lett.*, **96** (2006) 027005.
[18] Nishio T. *et al.*, *Phys. Rev. Lett.*, **101** (2008) 167001.
[19] Li S. C. *et al.*, *Appl. Phys. Lett.*, **89** (2006) 123111.
[20] Ma X. *et al.*, *Proc. Natl. Acad. Sci. U.S.A.*, **104** (2007) 9204.
[21] Homma Y. *et al.*, *Phys. Rev. B*, **62** (2000) 8323.
[22] Dynes C. *et al.*, *Phys. Rev. Lett.*, **41** (1978) 1509.
[23] Renner Ch. *et al.*, *Phys. Rev. Lett.*, **67** (1991) 1650.
[24] Sträßler S. *et al.*, *Phys. Rev.*, **158** (1967) 319.
[25] Özer M. M. *et al.*, *Phys. Rev. B*, **74** (2006) 235427.
[26] Schmidt V. V. *et al.*, *The Physics of Superconductors: Introduction to Fundamentals and Applications* (Berlin, Springer-Verlag) 1997.
[27] Özer M. M. *et al.*, *Nat. Phys.*, **2** (2006) 173.
[28] Anderson P. W., *J. Phys. Chem. Solids*, **11** (1959) 26.